2. A. R. Reinberg, Private communication.
3. "Techniques and Applications of Plasma Chemistry," John R. Hollahan and Alexis T. Bell, Editors, p. 22, Wiley-Interscience, New York (1974).
4. A. K. Sinha, H. J. Levinstein, T. E. Smith, G. Quintana, and S. E. Haszko, *This Journal*, 125, 601 (1978).
5. R. B. Bird, W. E. Stewart, and E. N. Lightfoot, "Transport Phenomena," p. 114, John Wiley & Sons, Inc., New York (1960).

Spectroscopic Analysis of the Interface Between Si and Its Thermally Grown Oxide

D. E. Aspnes*

Bell Laboratories, Murray Hill, New Jersey 07974

and J. B. Theeten

Laboratoire d'Electronique et de Physique, Limeil-Brevannes 94450, France

ABSTRACT

Spectroscopic ellipsometric data from 1.5-5.8 eV has been analyzed to determine the *in situ* optical response of the interface between Si and its thermally grown oxide. Results for <100>, <110>, and <111> sample orientations show an interface of width $d_{ox} = 7 \pm 2$Å consisting of atomically mixed Si and O of average stoichiometry $SiO_{0.4\pm0.2}$. The optical data are not consistent with either microroughness at the interface or an abrupt transition between crystalline Si and SiO_2 or a significant accumulation of amorphous Si at the interface, but rather support a gradual transition region. The thickness and the average λ5461 refractive index $n = 3.2 \pm 0.5$ of this region are in agreement with the fixed-wavelength results, $d \sim 6$Å and $n \sim 2.8$, of Taft and Cordes. The oxide on the <110> surface is shown to have a density about 1.2% less than that of corresponding oxides on <100> and <111> surfaces.

There has been much recent interest in studying the properties of the interface between Si and its thermally grown oxide, not only because of its technological importance but also because it is the chemically simplest, most easily managed semiconductor-oxide system and hence the one most likely to be understood in fundamental terms (1). Recent experimental results have been summarized by Wager and Wilmsen (2). In short, the interface is too narrow to be analyzed by conventional ion-milling techniques, which not only have inadequate depth resolution but also destroy the interface during the measurement process. The most reliable information has come from recent experiments using nondestructive techniques. Krivanek and co-workers (3) used transmission electron microscopy with 3Å resolution to show that the crystalline Si (c-Si) substrate terminates abruptly (within one monolayer) with a 4-8Å modulation of a period of 200-500Å. Rutherford backscattering (RBS) was used by Feldman and co-workers (4) to show the existence of about two monolayers equivalent of excess Si, which could occur for example as two layers of nonregistered Si under stoichiometric SiO_2, or as a single nonregistered layer of Si together with ~5Å of SiO under stoichiometric SiO_2. Fixed-wavelength λ5461 null ellipsometry (NE) by Taft and Cordes (5) indicated an interface about 6Å wide of effective index about 2.8. XPS measurements on ultrathin or chemically profiled oxides show a gradual transition region ~5Å (6) or 7-10Å (7) with evidence that the SiO_2 bonding is affected up to 40Å from the interface (6).

In this paper, we present results of a spectroscopic ellipsometric investigation of the Si-SiO_2 interface from 1.5 to 5.8 eV. Our objective was to take advantage of the sensitivity of ellipsometry to thin films and of the widely different dielectric properties of c-Si, amorphous Si (a-Si), SiO_2, and their mixtures in the visible-near u.v. spectral region to perform *in situ* spectroscopy on the protected interface and to determine information about its microstructure and chemical bonding from its visible-near u.v. optical response. TEM, RBS, and NE can provide general information about microstructure, but not about chemical bonding which requires some form of spectroscopy. XPS in principle can provide the latter information, but its interpretation is dependent on electron escape depths. Because spectroscopic ellipsometry does not depend on transport assumptions, requires only a transparent ambient (as, for example, SiO_2), and is sensitive to monolayers, it is a natural technique to apply to this problem. The results demonstrate also that spectroscopic ellipsometry can be used to study layers as thin as a few angstroms even though buried under hundreds or even thousands of angstroms of transparent overburden.

Analysis of the ellipsometric data shows that the interface is best represented as a 7 ± 2Å region of Si and O of average stoichiometry $SiO_{0.4\pm0.2}$. These data show clearly that the mixing is on a atomic scale rather than occurring as regions identifiable explicitly as a-Si and SiO_2 as might be expected from microroughness or incomplete oxidation of particulate material. Also rejected is an abrupt junction between Si and SiO_2 or an accumulation of a-Si at the interface. No difference in the interface region is observed for the three different interface orientations investigated here, although the SiO_2 overlayer on the <110> interface is about 1.2% less dense than that on the <100> or <111> interfaces. The microstructure that emerges is a laterally uniform, graded transition region of atomically mixed Si and O of thickness and composition as mentioned above. The results are consistent with the RBS alternative of a monolayer of a-Si followed by 5Å of SiO. The graded nature is in agreement with XPS measurements (6, 7). Finally, because the λ5461 refractive index of $SiO_{0.4\pm0.2}$ is 3.2 ± 0.5, the present results are also in agreement with the fixed-

* Electrochemical Society Active Member.
Key words: silicon, SiO_2, interface, ellipsometry.

wavelength λ5461 null ellipsometric measurements of Taft and Cordes (5). Thus a completely consistent picture is obtained.

Experimental

Spectroscopic ellipsometer.—The spectroscopic rotating-analyzer ellipsometer (RAE) used to obtain these data has been discussed in detail elsewhere (8). In brief, the essential features include a Xe 75W short-arc source for high luminosity and efficient collection at relatively low power dissipation, a Cary 14 spectrometer for excellent scattered light rejection, quartz Rochon prisms for extended spectral range and source/detector depolarization, and computerized Fourier processing of the digitized detector output for high precision. The detector circuit includes a feedback loop to achieve system linearity to at least one part in 10^3 over the entire operating range. A shutter periodically interrupts the lamp output to allow component drift and stray light contributions to be evaluated and eliminated at each wavelength. The data are corrected (9) for the optical activity of the quartz Rochon prisms.

While precision of a few parts in 10^5 is achieved routinely accuracy limits are more difficult to assess. Nevertheless, the following observations are suggestive. In straight-through operation, the calculated polarization plane is constant to within ±0.02° from 1.5 to 5.8 eV. Over the same range, the apparent a-c/d-c ratio is constant to within ±0.001. At a fixed wavelength, the analyzer and polarizer azimuths track to within ±0.01° over the ranges used, showing that the polarizer divided circle drive and the detector system is linear, and that source/detector residual polarization effects are negligible. Finally, calibration for a variety of samples routinely yields plane-of-incidence azimuths which are invariant to within ±0.05°, showing accurate reproducibility for sample alignment and also accurate compensation for the optical activity of the quartz Rochon prisms. Thus in direct angular measurements, the present photometric system is comparable to that of a good null ellipsometer, but somewhat less accurate than the ±0.01° fixed-wavelength instrument used by Taft and Cordes (5). The a-c/d-c ratio uncertainty has no direct analog in null ellipsometry, but corresponds roughly to an uncertainty of ±0.1° in ψ under worst-case conditions where the light leaving the sample is linearly polarized. These uncertainties are not large enough to affect the conclusions reached here on the basis of the data.

Sample preparation.—Three n-type single crystal Si wafers of 24-29 Ω cm resistivity and <100>, <110>, and <111> surface orientations were Syton polished to provide high quality specular surfaces. The wafers were precleaned by standard gate-oxide procedures, then cleaning oxides were grown in dry O_2 at 1000°C to a <111> thickness of 1000Å. These oxides were stripped, and final oxides were regrown under the same conditions to a <111> thickness of about 2000Å. All three wafers were processed simultaneously to eliminate any possible differences due to slight variations in processing and growth conditions. All processing was done on equipment used routinely for the production of high quality gate oxides.

The resulting oxides on the <100> and <111> wafers were about 2100 and 2300Å thick, respectively, and appeared absolutely uniform on visual inspection, although ellipsometric measurements showed a slight (5Å) nonuniformity in thickness over the wafers. The substantially thicker 2800Å <110> oxide showed an obvious thickness gradient over part of the surface, but about half the wafer was found to be sufficiently uniform for interface determinations to be performed.

To provide self-consistency checks, and particularly to establish conditions (10) for determining accurately individual model parameters such as the density of the SiO_2 overlayer, the samples were etched after the initial measurements to obtain further data at several different oxide thicknesses. We used a 5% HF-95% H_2O solution (5), which was observed to etch the <100>, <110>, and <111> sample oxides at 190, 120, and 200 Å/min, respectively. The <110> oxide also exhibited a different density than the <100> and <111> oxides, as is discussed below.

Data Processing

Determination of sample parameters.—Our general data reduction procedure has been discussed elsewhere (11). Briefly, we measure the complex reflectance ratio (optical impedance) of a composite sample from 1.5-5.8 eV and then compare these data objectively to model spectra calculated for a given hypothetical configuration by using standard equations (12) and linear regression analysis (13). The specific configuration studied here consists of a c-Si substrate, a possible interface, an oxide overlayer, and the air ambient. These constituents can be described by means of dielectric functions, thicknesses, possible void fractions and birefringence in the oxide, etc.

Because a single-wavelength ellipsometric measurement provides only two constraints, the parameters of the composite system are hopelessly underdetermined unless further conditions can be established. We generate the necessary constraints by making spectroscopic measurements and by including spectrally dependent and independently measurable data, such as the dielectric response of c-Si and SiO_2, as known quantities. This leaves only a few spectrally independent parameters such as oxide thickness to be determined by comparing model spectra to measured spectra. Thus a given model becomes highly overdetermined, and its validity can be judged readily by how well it fits the entire spectrum, not just at a single wavelength. Linear regression analysis (13) provides an objective and systematic way of minimizing the differences between the data and spectra computed for specific models and expressing the result in terms of best-fit model parameters and the unbiased estimator, $\hat{\sigma}$, of the mean square deviation, δ. We have shown previously (11) that linear regression analysis can be applied in this context not only as a systematic means of providing best-fit parameters, but also as a means of establishing correlations and confidence levels to show which parameters are well determined by the data and consequently should be emphasized and which parameters cannot be well determined by the data and consequently should be ignored.

Dielectric function data of constituents.—*c-Si substrate.*—No previously published c-Si dielectric function data exist that are sufficiently accurate and/or cover a sufficiently wide energy range to determine interface parameters. The best available low energy data are those of Hulthèn (14), determined below 3 eV by transmission measurements. The best wide-range data are those of Philipp (15), determined by Kramers-Kronig analysis of complex reflectance measurements, from 0-27 eV, with subsequent correction for the effect of oxide overlayers. The Hulthèn data are probably sufficiently accurate but do not cover an adequate spectral range. The Philipp data are probably accurate with respect to general amplitude values but are not available over a sufficiently fine grid and consequently show substantial shifts of threshold energies for interband transitions.

Accordingly, a c-Si spectrum was generated by accurately measuring the pseudodielectric function of a piece of the oxidized <110> sample that had been stripped in HF. Although the traditional approach is to correct these data by mathematically removing an overlayer of SiO_2, consistent interface results could be achieved only by mathematically removing the self-consistent 6Å overlayer of chemically mixed $\sim Si_{0.75}(SiO_2)_{0.25}$ that was determined by the interface analysis itself. This is in qualitative agreement with the results of Philipp (15), who noted previously that

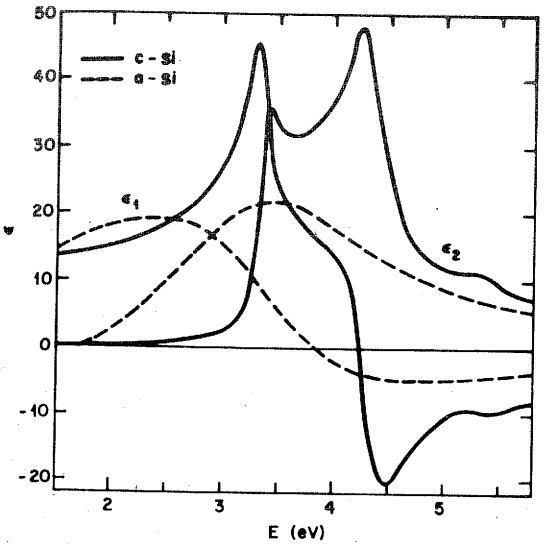

Fig. 1. Dielectric functions of c-Si and a-Si

the presence of an SiO_2 overlayer on stripped c-Si would lead to reflectance structure near 10 eV that is not observed.

Our resulting spectra are shown in Fig. 1. The ϵ_1 spectrum below the direct gap agrees with that of Hulthèn (14) to within 1½% and with that of Philipp (15) to within ½%. The maximum value of ϵ_2, 47.87, is slightly less than Philipp's value, 48.25, in agreement with discrepancies observed for Ge (16). Finally, the ϵ_2 values below the direct gap, which are exceptionally difficult to determine with an RAE, agreed with Hulthèn values to within 3%. However, because the transmission data are more accurate, our ϵ_2 data were replaced with Hulthèn's data below 2.5 eV. We thus believe these data to be the most accurate ever determined for c-Si over the visible-near u.v. quartz-optics range.

SiO_2 oxide.—The data base is the dispersion equation determined by Malitson (17) for fused silica. Taft (18) has shown that thermally grown oxides on c-Si differ at λ5461 from the Malitson data in at least two significant respects. First, thermally grown oxides show birefringence. Second, the index values depend on the growth temperatures and slightly on crystal orientation (only <100> and <111> data were given). The birefringence was shown (18) to arise entirely from the compressive stress in the thermally grown oxide, which in turn derives almost entirely from the mismatch in thermal expansion coefficients (19). Less clear is the origin of the index differences, which below 1200°C growth temperatures suggest the presence of different SiO_2 polytypes (18) and thus may not be related entirely to density differences.

For simplicity, we suppose that refractive index differences between our oxides and Malitson's data arise from density differences, which can be described accurately in the Bruggeman effective medium approximation (20). But this implies an assumption about the nature of the SiO_2 dispersion which presently cannot be tested. However, such effects do not appear to be important as is discussed more fully later.

Birefringence in the SiO_2 overlayer is incorporated by supposing different threshold shifts, $+\Delta E$ and $-0.5\,\Delta E$, for p- and s-wave polarizations, respectively, in the two higher energy Sellmeyer oscillators in the Malitson expression. The value $\Delta E = +0.017$ eV was chosen to give $n_e - n_o = 0.0007$ at λ5461 in agreement with the accurate measurements of Taft and Cordes (5). The effect on the complex reflectance ratio in model calculations was included by standard equations (12, 21).

Si-SiO_2 interface.—To determine the interface composition we require dielectric function spectra for the complete range $Si_x(SiO_2)_{1-x} = SiO_{2-2x}$, $0 \lesssim x \lesssim 1$. Experimental spectra are not available, but suitable interpolations can be obtained as follows.

First, we recognize two possible types of mixtures: physical, where optically identifiable regions of a-Si and SiO_2 coexist as, *e.g.*, microroughness or inclusions and host, on a scale small compared with the wavelength of light, and chemical, where the Si and O are mixed on an atomic scale. The former case is described by heterogeneous dielectric theory. We use the Bruggeman model together with data for a-Si that we obtained previously (22) and which are also shown in Fig. 1. The Malitson dispersion equation is used for SiO_2.

Specifically, the Bruggeman approximation (20) gives the effective dielectric function, $\langle\epsilon\rangle$, of a heterogeneous material as

$$0 = f_a\frac{\epsilon_a - \langle\epsilon\rangle}{\epsilon_a + 2\langle\epsilon\rangle} + f_b\frac{\epsilon_b - \langle\epsilon\rangle}{\epsilon_b + 2\langle\epsilon\rangle} + f_v\frac{1 - \langle\epsilon\rangle}{1 + 2\langle\epsilon\rangle} \quad [1]$$

where f_x, ϵ_x, x = a, b, v are the volume fractions and dielectric functions of the separate phases a, b, and v = void, respectively; $f_a + f_b + f_v = 1$. For the interface, we take $f_v = 0$. Because the volume associated with an SiO_2 molecule is 1.55 times larger than that associated with an Si atom in a-Si, the relation between atomic fraction x and the parameters of Eq. [1] are

$$\epsilon_a = \epsilon_{a\text{-}Si};\quad f_a = x/[x + 1.55(1 - x)] \quad [2a]$$

$$\epsilon_b = \epsilon_{SiO_2};\quad f_b = 1.55(1 - x)/[x + 1.55(1 - x)] \quad [2b]$$

Spectra calculated for x in increments of 0.125 are shown in Fig. 2.

Spectra for chemically mixed Si and O are calculated in a model that we developed previously for another application and which is completely described elsewhere (23). Results for x values in increments of 0.125 are also shown in Fig. 2. The physical and chemical models differ in that the peak value of ϵ_2 remains at 3.5 eV until a relatively large SiO_2 fraction is present in the former case, but immediately starts shifting to higher energies with increasing O content in the latter case. This is a result of the electronegativity difference between Si and O which moves the average oscillator strength to higher energies in the blended material. Also, boundary screening inhibits the dilution effect of O in physical mixtures, requiring more O to achieve a given reduction in the long-wavelength refractive index than for atomically mixed material. The qualitative difference can be seen immediately by comparing the spectra for the $x = 0.75$ physically mixed and $x = 0.875$

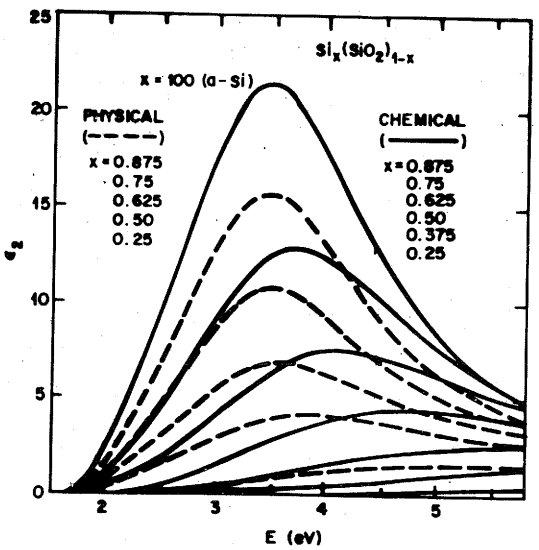

Fig. 2. Comparison of ϵ_2 spectra for physical and chemical mixtures of a-Si and SiO_2 for atomic fractions of a-Si in SiO_2 as indicated.

chemically mixed materials, which are essentially identical up to 3 eV and differ appreciably only in the u.v. Both cases have been observed: the former behavior describes spectra (24) of the composite material SIPOS, while the latter describes the atomically mixed material evaporated silicon monoxide (25).

We reemphasize that physical and chemical mixtures cannot be distinguished optically without determining the dielectric response in the near u.v. Thus the n = 2.8 value for the interface at λ5461 obtained by Taft and Cordes (5) corresponds to either a physical mixture of $x = 0.65$ or a chemical mixture of $x = 0.73$. No further information can be obtained at a single wavelength.

Results

1-, 2-, and 3-parameter models.—Typical tan ψ, cos Δ data for an oxidized Si wafer of <100> orientation and oxide thickness 1360Å are shown in Fig. 3. These data exhibit the characteristic interference pattern with increasing energy as the optical standing waves in the oxide pass through increasing periods. Interface sensitivity is maximized for the p- and s-wave components near minima and maxima, respectively, in tan ψ as minimum reflectance implies maximum energy density at the interface as previously discussed (11, 26).

The results of least squares fitting 1-, 2-, and 3-parameter models to these data are shown in Fig. 4. The fitting was done at 83 points equally spaced over the 1.5-5.8 eV interval to the real and imaginary parts of ρ calculated from tan x and cos Δ. Rather than compare spectra directly in terms of tan ψ and cos Δ, we show the differences because in every case these are small and would not be seen on the scale of Fig. 3.

Figure 4 shows that a one-parameter model consisting of an ideal c-Si substrate, no interface, and an ideal SiO_2 overlayer does not reproduce accurately the peak in tan ψ. For this model the least squares procedure yields $d_{ox} = 1368.6 \pm 0.4$Å and $\hat{\sigma} = 0.0567$. The uncertainty shown here, and those which follow, refer to 90% confidence limits based on the mismatch between model spectra and data and do not include possible systematic errors. By allowing the void volume density to vary, most of the tan ψ discrepancy near 2 eV disappears although the phase spectrum, cos Δ, and the higher tan ψ mismatch are not improved. The parameters obtained in this two-parameter model are $d_{ox} = 1363.6 \pm 0.3$Å, void fraction $f_v = -0.0062 \pm 0.0004$, and $\hat{\sigma} = 0.0166$. Thus the fit as measured by $\hat{\sigma}$ is improved significantly, by more than a factor of 3. The negative void fraction simply means that the thermally grown oxide is effectively more dense than the fused-quartz reference, a result that has been well characterized for oxides on <100> and <111> wafers (18).

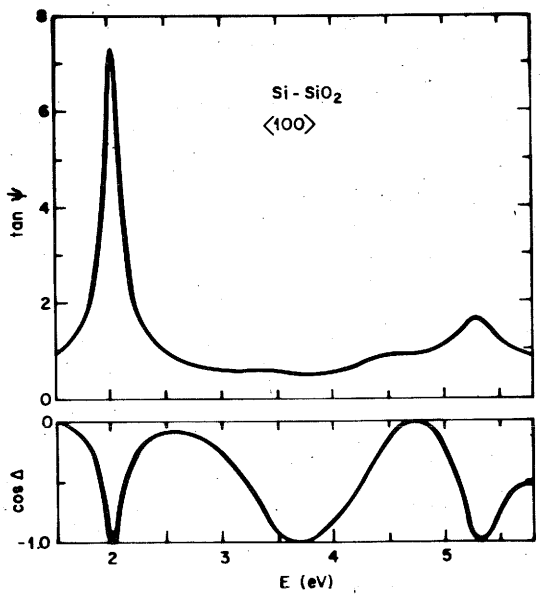

Fig. 3. Typical tan ψ, cos Δ data for an oxidized Si wafer. The orientation is <100> and the oxide thickness is 1360Å.

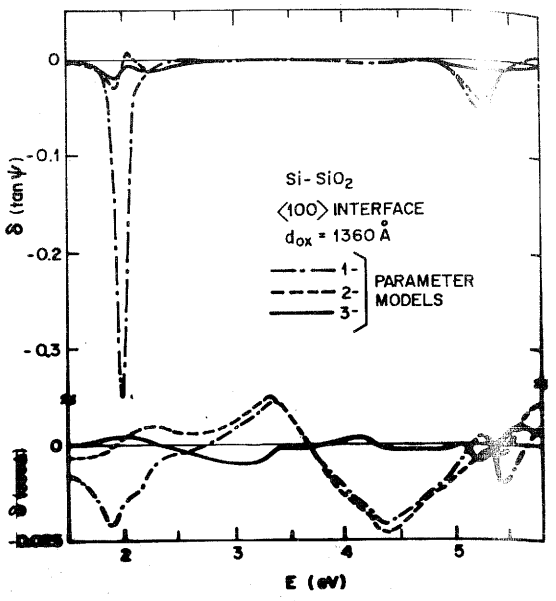

Fig. 4. Differences between theoretical and experimental tan ψ and cos Δ spectra for 1-, 2-, and 3-parameter models of the <100> SiO_2 interface for an SiO_2 overlayer of approximately 1360Å.

In terms of an equivalent refractive index at λ5461, where $n_0 = 1.4602$ for fused quartz, the above void fraction corresponds to $n = 1.4631 \pm 0.0002$. This is less than the Taft value of 1.4678 obtained for <100> samples oxidized in dry O_2. Lower values obtain if traces of H_2O are present in the oxidizing atmosphere (18), whence the result is physically reasonable. Note that the thickness has decreased as n has increased to maintain the optical thickness, nd, essentially unchanged. The two-parameter model as used here includes birefringence, although its effect is relatively minor.

By incorporating an interface of chemically mixed $Si_{0.75}(SiO_2)_{0.25}$, the periodic discrepancy between data and model computations for cos Δ and the remaining 5 eV discrepancy for tan ψ are both largely eliminated. Specifically, we find $d_{ox} = 1359.9 \pm 0.5$Å, the interface thickness $d_{int} = 6.6 \pm 0.9$Å, $f_v = -0.0065 \pm 0.0002$, and $\hat{\sigma} = 0.0098$ in this three-parameter model. Thus the presence of an interface improves the overall fit by nearly another factor of 2. The void fraction is essentially unchanged but d_{ox} has decreased by nearly 4Å, showing that the oxide is trying to simulate the effect of the interface in the two-parameter model. The above improvement constitutes the existence proof for the interface.

Interface composition and thickness.—Having dielectric function spectra for the possible interface compositions, one can now use linear regression analysis in a 4-phase model with three free parameters (d_{int}, f_v, d_{ox}) to determine the "best" interface. Figure 5 shows the variation of $\hat{\sigma}$ for three oxide thicknesses on the <100> sample for the full range of interface composition $Si_x(SiO_2)_{1-x}$ from no interface ($x = 0$) to pure a-Si ($x = 1$) for both chemical and physical mixture models. Generally speaking, a consistent set of values of d_{ox}, d_{int}, and f_v was obtained near the residual minimum for each oxide thickness, although values away from the minimum showed wide variations as the least squares approach attempted to compensate the interface compositional error imposed by the model through various combinations of the three free parameters.

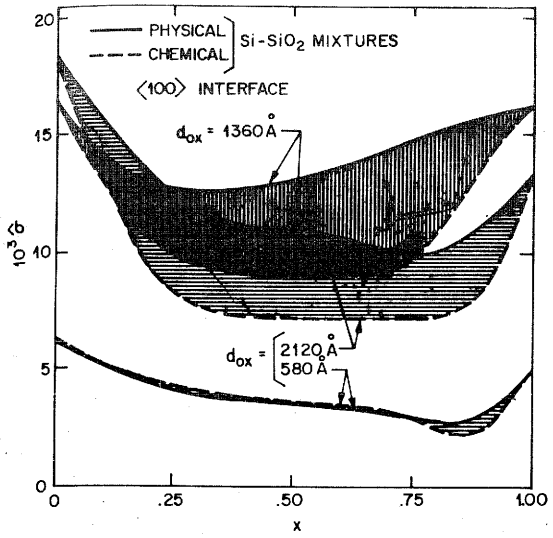

Fig. 5. Variation of 3-parameter 4-phase model residuals with interface composition for <100> Si-SiO_2 interface for SiO_2 overlayers of approximately 580, 1360, and 2120Å. Limits corresponding to physical and chemical mixtures are shown.

Conclusions immediately obvious from Fig. 5 are as follows. First, an interface is present, in agreement with previous work (1-7). $\hat{\sigma}$ always decreased for a finite interface, regardless of oxide thickness or assumed interface composition. Second, a chemically mixed Si-O interface gives better results than a physical mixture of Si and SiO_2. For the orientation shown, the difference is greatest for the thicker oxides although this is not generally true. Third, the statistically favored interface composition range is approximately $0.3 < x < 0.8$ based on Fig. 5.

The relatively broad compositional range allowed by Fig. 5 can be narrowed significantly by requiring consistency of the free parameters determined by the individual least squares fits on samples that differ only by etching the oxide to new thicknesses. In this context d_{ox} is clearly a meaningless parameter. However, f_v is the key to the analysis because its value is determined at $d_{ox} \sim 1400$Å with an order-of-magnitude less sensitivity to interface properties than at other thicknesses, owing to a particular favorable combination of parameters and measurement conditions (10). This occurs because of exceptionally good impedance-matching characteristics for s-wave polarization near 2 eV for the given combination of materials and measurement conditions, which for the small interface thicknesses used here depends almost entirely on the refractive index of the oxide overlayer. The independence on interface composition can be understood immediately by noting that at 2 eV all mixtures are transparent, as shown in Fig. 2.

If one requires that the values of f_v determined for overlayer thicknesses near 1400Å must also apply at other thicknesses, the results shown in Table I are obtained. Here, df_v/dx is calculated from least fit spectra for $x = 0.625$, 0.75, and 0.875, and the interpolated values of x obtained by requiring all f_v values to be equal to that at $d_{ox} \sim 1400$Å, for which $df_v/dx \cong 0$, are also shown. Uncertainties in x are calculated from equivalent uncertainties in f_v. The values of d_{int} are then obtained by interpolation from solutions for $x = 0.625$, 0.75, and 0.875.

The results of the analysis are shown in Table I and plotted in Fig. 6 and 7. We repeat that the error bars shown derive from 90% confidence levels based on the fits of specific models to the data, and do not include systematic errors. Nevertheless, all data are consistent with an interface 7 ± 2Å wide composed of a chemical (atomic) mixture of Si and O of average stoichiometry

Table I. Interface compositions determined by requiring consistency in f_v among all data for a given sample. Due to insensitivity to interface parameters, the value of f_v for $d_{ox} \approx 1400$Å is chosen as reference unless otherwise noted by parentheses (see text).

Sample	d_{ox} (Å)	df_v/dx	f_v	x	d_{int} (Å)
<100>	2120	−0.028	−0.0065 ± 0.0002	0.78 ± 0.06	8.3 ± 1.0
	1360	−0.003		(0.75)	6.6 ± 0.9
	584	−0.016		0.81 ± 00.3	5.4 ± 0.9
<111>	2282	−0.028	−0.0059 ± 0.0008	0.83 ± 0.08	7.7 ± 1.4
	1445	−0.002		(0.75)	6.0 ± 3.7
	659	−0.023		0.83 ± 0.06	6.0 ± 1.1
<110>	2805	−0.034	+0.0065 ± 0.0005	0.74 ± 0.06	8.3 ± 1.5
	2318	−0.037		(0.75)	9.6 ± 1.5
	2142	−0.031		0.82 ± 0.05	8.8 ± 1.1
	1407	0.000		(0.75)	4.7 ± 2.1
	604	−0.014		0.91 ± 0.09	6.3 ± 3.4

$Si_{0.8\pm0.1}(SiO_2)_{0.2\pm0.1} \cong SiO_{0.4\pm0.2}$. The three points corresponding to $d_{ox} \sim 1400$Å are shown without error bars in Fig. 7 because they cannot be determined from f_v and the residual minimum (see Fig. 4) is too broad to yield a definitive result. All three actually have a weak residual minimum near $x = 0.6$, but this value is not consistent with the well-defined values obtained at other oxide thicknesses. In deference to this tendency we have shaded the average x value slightly to lower values for these points. A second <110> point also failed to provide an f_v value consistent with the re-

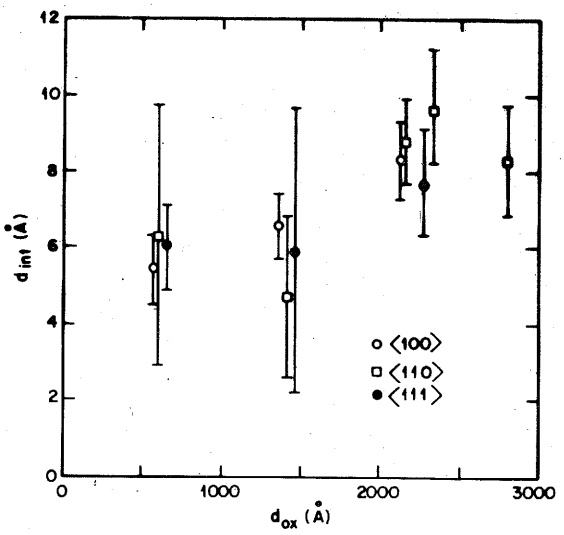

Fig. 6. Calculated interface thicknesses for <100>, <110>, and <111> samples after initial growth and at various stages of etching, from Table I.

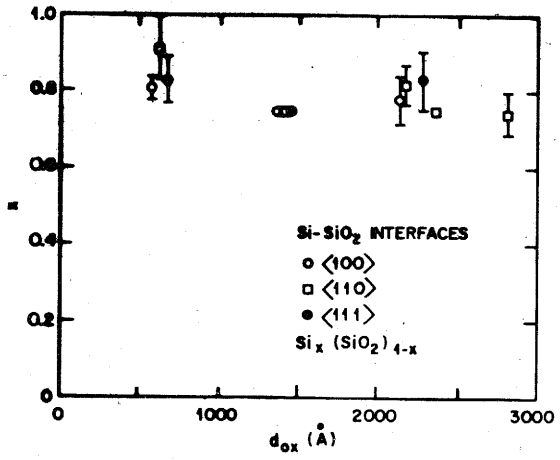

Fig. 7. Calculated interface composition x in chemically mixed $Si_x(SiO_2)_{1-x}$ after initial growth and at various stages of etching, from Table I.

maining data. Its contribution was defined similarly and its datum also shown in Fig. 7 without error limits.

The values of interface width determined here agree with that given in our initial report (11), which discussed data obtained on a single sample at a single value of oxide thickness. The uncertainty in the previously determined stoichiometry, SiO, could not be established from the single-thickness data and should be considered as superceded by the present results. All work, however, supports the conclusion that the interface Si and O are atomically mixed.

Discussion

Systematic errors.—If the data and analysis were exact and totally self-consistent, the interface parameters would be invariant with respect to oxide thickness and the residuals would reach negligibly small values. It is clear that this ideal has been approached but not completely reached; while the compositional data of Fig. 7 are reasonably constant, the results given in Fig. 6 show a trend of decreasing interface thickness as the oxide overlayer is gradually removed by etching. Because the interface is protected and cannot be affected by etching, this suggests that a small systematic error may be present.

The most probable sources of systematic errors are instrumental accuracy, nonuniformity (either in thickness or composition) of the oxide overlayer both in the as-grown and etched conditions, the ϵ spectrum for c-Si, or the ϵ spectrum for SiO_2. In self-consistent tests we have shown that the instrument accuracy approaches null ellipsometer accuracy as discussed in the Experimental section. Taft and Cordes have discussed the oxide uniformity problem at length and have concluded that the overlayer is uniform to the extent needed to analyze the interface problem (5). Moreover, their data show clearly that the etching procedure used there (and followed here) yields consistent results for 200Å increments from 7000Å to zero.

We next consider the ϵ data bases. With respect to that of c-Si, the effect of removing mathematically compositions and thicknesses from the stripped <110> sample data other than the self-consistent 6Å of chemically mixed $\sim Si_{0.75}(SiO_2)_{0.25}$ has been examined. No difference results if physically mixed spectra are used in place of chemically mixed spectra. Decreasing the removed thickness causes a general shift of all interface widths to lower values but does not affect either the trend or the conclusion that a chemically mixed interface is preferable to a physically mixed interface. Thus in principle the width data are subject to a general systematic uncertainty of no more than 2Å depending on possible future improvements of the ϵ data for c-Si. But we do not feel the possibility likely because of the agreement of the ϵ data with the Hulthèn and Philipp work as discussed in the section on Data Processing, and the fact that our interface results agree at λ5461 with those of Taft and Cordes.

We are left with the SiO_2 ϵ data. Taft has shown that the n values at λ5461 cannot be described below 1200°C as a simple compression of fused quartz and has suggested that other polymorphs of SiO_2 may be present in the oxide (17). Because these polymorphs should have different absorption thresholds and/or oscillator strengths, this implies that the Malitson dispersion equation will have only approximate validity: the dispersion in ϵ_1 at higher energies for thermally grown oxides may well deviate from the Malitson values. In principle, if sufficiently thick oxides can be grown this hypothesis can be checked directly with spectroscopic ellipsometry by reducing the data for the oxide ϵ_1 values assuming the presence of a known substrate and interface. If the oxide thickness approaches 1 micron, one could expect that the spectra are dominated by the oxide and that substrate and interface discrepancies would be minor.

A better SiO_2 representation was attempted by reducing the 2120Å <100> oxide data within the three-phase model and fitting the resultant spectrum to a three-term Sellmeyer oscillator with energies at the Malitson values and using the amplitudes as free parameters. The smoothly varying Sellmeyer terms average over the interference oscillations arising from the interface and extract the background, which is the intrinsic response of SiO_2. The results showed amplitudes of 12.73 ± 0.35, 4.36 ± 0.18, and 0.17 ± 0.10 eV for the oscillators at 18.2, 10.67, and 0.125 eV, respectively, compared to the Malitson values 12.617, 4.351, and 0.112 eV. The differences are not statistically significant, although the trend indicates a shift of the oxide absorption edges to lower energy. But the revised values changed interface thickness values by less than a few percent and did not affect the systematics of the results. Therefore, oxide effects alone appear to be ruled out.

Thus systematic errors cannot be traced to individual sources but rather may be an accumulation of effects from several sources. A further assignment of their origin would require more accuracy than presently attainable.

Microscopic structure of the interface.—The unusual effective average composition $SiO_{0.4\pm0.2}$ suggests that the layer whose effective thickness is 7 ± 2Å is actually graded in composition (6, 7), though laterally uniform. The connection between effective average and actual position-dependent dielectric functions, where the spatial variation is restricted to one dimension, has been considered in many contexts and most recently by Plieth and Naegele (27). In short, the spatial dependence can be replaced by a spatial average if the region is sufficiently thin, as is the case here. Specifically, for a thin layer on a uniform substrate (three-phase model) the change in the complex reflectance ratio is given by

$$\rho = \rho_0 \left\{ 1 + \frac{4\pi i n_a d \cos\phi}{\lambda} \frac{\epsilon_s(\epsilon_s - \epsilon_0)(\epsilon_0 - \epsilon_a)\sin^2\phi}{\epsilon_0(\epsilon_s - \epsilon_a)[\epsilon_s\cos^2\phi - \epsilon_a\sin^2\phi]} X \left[1 - \frac{\epsilon_a\epsilon_0\epsilon_s}{(\epsilon_s - \epsilon_0)(\epsilon_0 - \epsilon_a)} \delta\epsilon \right] \right\} \quad [3]$$

where ϵ_s and $\epsilon_a = n_a^2$ are the dielectric functions of the uniform substrate and ambient, respectively, and

$$\epsilon_0 = \frac{1}{d}\int_{-d}^{0} dz\epsilon(z) \quad [4a]$$

$$\delta\epsilon_0 = \frac{1}{d}\int_{-d}^{0} dz[\epsilon^{-1}(z) - \epsilon_0^{-1}] \quad [4b]$$

It is supposed that the nonuniform response extends only over $-d < z < 0$.

The term involving $\delta\epsilon_0$ is a correction that does not appear in the classical three-phase model, that is, if the dielectric response of the interface is spatially invariant. If the interface is graded, it arises because the functional dependence on $\epsilon(x)$ of the wave equation for p-polarization is different from that for the s-polarization, leading to a different weighting in the spatial average (27). We express it as in Eq. [3] to estimate more easily its relative effect. Using the data of Fig. 1 and 2, it is straightforward to show that its magnitude is of the order of 0.2 for an assumed linear variation in dielectric response. Since we are concerned only with estimating possible limits to the variation, this is small enough to be neglected and the effective dielectric response obtained in the previous section can be taken to be the simple spatial average of the actual variation.

We consider next the probable location of the interface as determined by optical measurements. The interface is operationally defined as that region whose optical response is measurably different from that of the c-Si substrate and the SiO_2 overlayer. Considering the c-Si side first, the atoms in the outermost c-Si plane

have neither lattice nor lateral symmetry because they are bonded on one side to the adjacent disordered region. Moreover, at least some of those atoms will be involved in oxygen bonding to the disordered region even though the total oxygen concentration there may be small. Their dielectric response should therefore be more like a-Si than c-Si. Thus optical measurements would view the interface as containing the outermost c-Si plane. On the SiO_2 side, the optical interface would terminate before full stoichiometry is reached because, by Fig. 2, it is not possible to distinguish between $SiO_{1.5}$ and SiO_2 in the 1.5-6.0 eV region with presently attainable accuracy. We should not expect to distinguish from SiO_2 a possible slightly perturbed ~40Å SiO_2 region as suggested by XPS measurements (6). As mentioned earlier, the preference for chemical, rather than physical, mixing rules out microroughness and the possibility of small Si inclusions near the interface resulting from nonuniform oxidation.

From the spatial average argument, Fig. 2, and the results of the preceding section, it is apparent that no more than one-third (~2Å) of the interface could appear as a-Si if the remainder were at least as oxygen-rich as SiO. We can reject the case of a-Si followed by stoichiometric SiO_2 because the optical data would have shown a narrower interface, and in any event a-Si is not the favored stoichiometry. Thus the accumulation of a-Si at the interface does not occur. Because the outermost ~c-Si plane is fulfilling optically the function of an a-Si layer, we are left with a region that is effectively about 5Å of SiO, in agreement with one of the RBS alternatives. Although the interface is undoubtedly graded, the width is small enough for the spatial-average limit to be valid whence the optical data can provide no further information on its distribution.

We note finally that the average refractive index of the 7 ± 2Å region of $SiO_{0.4\pm0.2}$ at λ5461 is 3.2 ± 0.5, as compared to the Taft-Cordes λ5461 value of ~2.8 determined for their ~6Å interface. Thus the fixed-wavelength null ellipsometric and spectroscopic ellipsometric results are in agreement at the wavelength at which they overlap.

Acknowledgments

We thank E. Povilonis for kindly growing the oxide films used here. One of us (D.E.A.) wishes to thank H. R. Philipp for supplying a numerical listing of the c-Si ϵ data reported in Ref. (15).

Manuscript submitted Sept. 10, 1979; revised manuscript received Dec. 21, 1979.

Any discussion of this paper will appear in a Discussion Section to be published in the December 1980 JOURNAL. All discussions for the December 1980 Discussion Section should be submitted by Aug. 1, 1980.

Publication costs of this article were assisted by Bell Laboratories.

REFERENCES

1. See, for instance, "Physics of SiO_2 and Its Interfaces," S. T. Pantelides, Editor, Pergamon Press, New York (1978).
2. J. F. Wager and C. W. Wilmsen, *J. Appl. Phys.*, **50**, 874 (1979).
3. O. L. Krivanek, D. C. Tsui, T. T. Sheng, and A. Kamgar, in "Physics of SiO_2 and Its Interfaces," S. T. Pantelides, Editor, p. 356, Pergamon Press, New York (1978).
4. L. C. Feldman, P. J. Silverman, J. S. Williams, T. E. Jackman, and I. Stensgaard, *Phys. Rev. Lett.*, **41**, 1396 (1978); L. C. Feldman, I. Stensgaard, P. J. Silverman, and T. E. Jackman, in "Physics of SiO_2 and Its Interfaces," S. T. Pantelides, Editor, p. 344, Pergamon Press, New York (1978).
5. E. Taft and L. Cordes, *This Journal*, **126**, 131 (1979).
6. F. J. Grunthaner and J. Maserjian, in "Physics of SiO_2 and Its Interfaces," S. T. Pantelides, Editor, p. 389, Pergamon Press, New York (1978).
7. S. I. Raider and R. Flitsch, in *ibid.*, p. 384.
8. D. E. Aspnes and A. A. Studna, *Appl. Opt.*, **14**, 220 (1975); in "Optical Polarimetry-Instrumentation and Applications," Vol. 112, R. M. A. Azzam and D. L. Coffeen, Editors, p. 62, SPIE, Bellingham, Wash. (1977); *Rev. Sci. Instrum.*, **49**, 291 (1978).
9. D. E. Aspnes, *J. Opt. Soc. Am.*, **64**, 812 (1974).
10. J. B. Theeten and D. E. Aspnes, *Thin Solid Films*, **60**, 183 (1979).
11. D. E. Aspnes, J. B. Theeten, and R. P. H. Chang, *J. Vac. Sci. Technol.*, **16**, 1374 (1979).
12. R. M. A. Azzam and N. M. Bashara, "Ellipsometry and Polarized Light," chap. 4, North Holland, Amsterdam (1977); D. E. Aspnes, in "Optical Properties of Solids: New Developments," B. O. Seraphin, Editor, p. 799, North-Holland, Amsterdam (1976).
13. E. S. Keeping, "Introduction to Statistical Inference," chap. 12, Van Nostrand, Princeton, N.J. (1962).
14. R. Hulthèn, *Phys. Scr.*, **12**, 342 (1975).
15. H. R. Philipp, *J. Appl. Phys.*, **43**, 2835 (1972).
16. D. E. Aspnes and A. A. Studna, in 1979 Ellipsometry Conference Proceedings, *Surf. Sci.*, In press.
17. I. H. Malitson, *J. Opt. Soc. Am.*, **55**, 1205 (1965). The dispersion equation actually used in these computations is that given in "American Institute of Physics Handbook," third edition, D. E. Gray, Editor, pp. 6-29, McGraw-Hill Book Co., New York (1973).
18. E. A. Taft, *This Journal*, **125**, 968 (1978).
19. R. J. Jaccodine and W. A. Schlegel, *J. Appl. Phys.*, **37**, 2429 (1966).
20. D. A. G. Bruggeman, *Ann. Physik (Leipzig)*, **24**, 636 (1935).
21. D. den Engelsen, *J. Opt. Soc. Am.*, **61**, 1460 (1971).
22. D. E. Aspnes, J. B. Theeten, and F. Hottier, *Phys. Rev.*, **820**, 3292 (1979).
23. D. E. Aspnes and J. B. Theeten, *J. Appl. Phys.*, **50**, 4928 (1979).
24. D. E. Aspnes, W. R. Knolle, and H. R. Maxwell, Jr., Unpublished.
25. H. R. Philipp, *J. Phys. Chem. Solids*, **32**, 1935 (1971).
26. J. B. Theeten, D. E. Aspnes, and R. P. H. Chang, *J. Appl. Phys.*, **49**, 6097 (1978).
27. W. J. Plieth and K. Naegele, *Surf. Sci.*, **64**, 484 (1977).